J|A|C|S
ARTICLES
Published on Web 09/25/2002

Electronic Properties of Polyoxometalates: Electron and Proton Affinity of Mixed-Addenda Keggin and Wells−Dawson Anions

Xavier López, Carles Bo, and Josep M. Poblet*

Contribution from the Departament de Química Física i Inorgànica and Institut d'Estudis Avançats, Universitat Rovira i Virgili, Imperial Tarraco 1, 43005 Tarragona, Spain

Received March 20, 2002

Abstract: A series of systematic DFT calculations were conducted on Keggin $[SiW_9M_3O_{40}]^{n-}$, M = Mo, V, and Nb; and Wells−Dawson anions $[P_2M_{18}O_{62}]$,$^{6-}$ M = W and Mo; $[P_2M_{15}M_3'O_{62}]^{m-}$, M = W and Mo, M′ = W, Mo, and V to analyze the redox properties and the basicity of the external oxygen sites in polyoxometalates with nonequivalent addenda metals. The energy and composition of the lowest unoccupied orbitals, formally delocalized over the addenda atoms, determine the redox properties of a polyoxometalate. When a Mo^{6+} substitutes one W^{6+} in the 1:12 tungstate, the energy of the LUMO decreases and the cluster is more easily reduced. The tungstoniobates behave differently because the niobium orbitals insert into the tungsten band and the reduction of $[SiW_9Nb_3O_{40}]^{7-}$ yields the *blue* species SiW_9Nb_3 1e and not the cluster $SiW_9Nb_2Nb^{IV}$. In Wells−Dawson structures, the polar and equatorial sites have different electron affinities and the reduction preferentially occurs in the equatorial sites. Inserting ions with larger electron affinities into the polar sites can modify this traditional conduct. Hence, the trisubstituted $[P_2W_{15}V_3O_{62}]^{9-}$ anion is reduced in the vanadium polar sites. By means of molecular electrostatic potential maps and the relative energy of the various protonated forms of $[SiW_9V_3O_{40}]^{7-}$ and $[SiW_9Mo_3O_{40}]^{4-}$, we established the basicity scale: OV_2 > OMo_2 > OW_2 > OV > OW > OMo. Finally, a continuum model for the solvent enabled us to compare anions with different total charges.

Introduction

Polyoxometalates[1,2] (POMs) and their transition-metal-substituted derivatives are a large group of transformable anionic clusters that have multiple applications, many of which are related to their redox properties.[3] POMs are structures that contain arrays of corner- and edge-sharing pseudo-octahedrally coordinated MO_6 units, packed to form an ionic core, where the electronic configuration of the metal is usually d^0 or d^1 and is commonly called *addenda* or *peripheral* element. The most typical addenda elements that form molecular (discrete) metal oxides are W^{VI}, Mo^{VI}, and V^V because their ionic radii and charge are suitable for combining with O^{2-}. Nonetheless, many POMs have been synthesized by incorporating (substituting or adding) other metallic centers. Among many other heteropoly architectures, Keggin anions[4] $[XM_{12}O_{40}]^{n-}$ and Wells−Dawson (W−D) anions[5] $[X_2M_{18}O_{62}]^{m-}$, as well as their derived aggregates, form a basic set of clusters that have given rise to a vast literature. In the formulation of heteropolyanions (HPAs), X is the *internal* element.[1]

The composition of the metal and the shape of the framework define the properties of a POM. For example, the improvement in the catalytic activity of polyanions is closely related to addenda substitution.[6] At the end of the 1960s, the work of C. Tourné and G. Tourné[7] created interest in how addenda substitution affected POMs, and this interest grew rapidly in the subsequent decades. Most research on the Lindqvist isopolyanion was carried out by Klemperer and co-workers[8,9] with the aim of obtaining suitable polyoxometalate-supported organometallic derivatives. Mixed-addenda HPA research is even more extensive since Keggin- and Dawson-type derivatives can give rise to a greater number of stoichiometries, shapes, and aggregates. The addenda W^{VI}, Mo^{VI}, V^V, and Nb^V and the main group heteroatoms P and Si are the most usual metal ions in Keggin and W−D HPAs, but other fourth (Ti,[6e,10] Zr[11]), fifth (Ta),[12] and sixth (Cr)[13] row transition-metal elements have been incorporated into the POM framework. Lanthanides, actinides,[14]

* Address correspondence to this author. E-mail: poblet@quimica.urv.es.

(1) Pope, M. T. *Heteropoly and Isopoly Oxometalates*; Springer-Verlag: Berlin, 1983.
(2) Hill, C. L., Ed. *Chem. Rev.* **1998**, *98*, 1−390 (Special Issue on Polyoxometalates).
(3) Katsoulis, D. E. *Chem. Rev.* **1998**, *98*, 359.
(4) Keggin, J. F. *Nature* **1933**, *131*, 908.
(5) (a) Dawson, B. *Acta Crystallogr.* **1953**, *6*, 113. (b) D'Amour, H. *Acta Crystallogr., Sect C.* **1976**, *32*, 729.
(6) See, for example: (a) Duncan, D. C.; Chambers, R. C.; Hecht, E.; Hill, C. L. *J. Am. Chem. Soc.* **1995**, *117*, 681 and references therein. (b) Cavani, F.; Koutyrev. M.; Trifirò, F. *Catal. Today.* **1996**, *28*, 319−333. (c) Kogan, V.; Aizenshtat, Z.; Neumann, R. *Angew. Chem., Int. Ed.* **1999**, *38*, 3331−3334. (d) Bagno, A.; Bonchio, M.; Sartorel, A. Scorrano, G. *Eur. J. Inorg. Chem.* **2000**, 17−20. (e) Kholdeeva, O. A.; Maksimov, G. M.; Maksimovskaya, R. I.; Kovaleva, L. A.; Fedotov, M. A.; Grigoriev, V. A.; Hill, C. L. *Inorg. Chem.* **2000**, *39*, 3828−3837. (f) Zeng, H.; Newkome, G. R.; Hill, C. L. *Angew. Chem., Int. Ed.* **2000**, *39*, 1771−1774 and ref 2 therein. (g) Khenkin, A. M.; Shimon, L. J.; Neumann, R. *Eur. J. Inorg. Chem.* **2001**, 789−794. (h) Nishiyama, Y.; Nakagawa, Y.; Mizuno, N. *Angew. Chem., Int. Ed.* **2001**, *40*, 3639−3641.
(7) Tourné, C.; Tourné, G. *Bull. Soc. Chim. Fr.* **1969**, 11244.
(8) Day, V. W.; Klemperer, W. G. *Science* **1985**, *228*, 533−541.

10.1021/ja020407z CCC: $22.00

and nontransition-metal derivatives have also been reported.[6b,g,15] A considerable number of traditionally paramagnetic atoms have been included in the framework of Keggin and W−D anions, as well as in the sandwich-type molecules[16] derived from them. This is a growing area in which rational methods for systematically modifying POM structures have still to be fully developed.[17]

In two previous papers, we showed that quantum chemistry calculations based on the DFT formalism may be very useful for understanding and rationalizing the electronic and magnetic properties of Keggin anions.[18,19] The systematic study of the series $[XM_{12}O_{40}]^{n-}$, where M is W or Mo and X is a main group element or a transition-metal ion, supported the hypothesis that a Keggin anion may also be viewed as a XO_4^{n-} anion inside a neutral cage, a decomposition that was useful in the analysis of the α/β isomerism in nonsubstituted Keggin anions.[19] DFT calculations also correctly described the redox properties in anions with transition-metal heteroatoms such as Co(II), Co(III), or Fe(III)[18,20] and their magnetic features.[21] In the present paper, we report a detailed DFT study on the series of anions A-α-$[SiW_9M_3O_{40}]^{n-}$, M = V(V), Nb(V), or Mo(VI); α-$[P_2M_{18}O_{62}]$,$^{6-}$ M = W(VI) or Mo(VI); α-$[P_2M_{15}M'_3O_{62}]^{m-}$, M = W(VI) or Mo(VI); and $[P_2M_{15}V'_3O_{62}]^{m-}$, M = W(VI) or Mo(VI) to analyze the redox properties and the basicity of the external oxygen sites in clusters with nonequivalent addenda. Only clusters preserving a three-fold axis were considered since three-substituted clusters are very frequent and usually the substitution takes place in three neighboring octahedra. Moreover, C_{3v} systems require less computational demands. Throughout the paper, we will generally use the shorthand notation without either oxygen atoms or charge. Thus, for example, P_2W_{18} denotes the fully oxidized $[P_2M_{18}O_{62}]^{6-}$ Wells−Dawson anion. $P_2W_{18}1e$ means that the cluster is single-reduced. These kinds of systems are also known as *blue* species.[1] Despite the enormous effort made in the last thirty years to synthesize and study the chemical properties in these molecule types,[22,23] we believe that their basic electronic properties still need to be systematically analyzed.

The Keggin structure may be viewed as the assembly of four M_3O_{13} edge-sharing triads (*B-triads*) or as the packing of four

(9) (a) Klemperer, W. G.; Shum, W. *J. Am. Chem. Soc.* **1977**, *99*, 3544. (b) Klemperer, W. G.; Shum, W. *J. Am. Chem. Soc.* **1978**, *100*, 4891. (c) Filowitz, M.; Ho, R. K. C.; Klemperer, W. G. *Inorg. Chem.* **1979**, *18*, 93. (d) Besecker, C. J.; Klemperer, W. G. *J. Am. Chem. Soc.* **1980**, *102*, 7598−7600. (e) Day, V. W.; Fredrich, M. F.; Thompson, M. R.; Klemperer, W. G.; Liu, R.-S.; Shum, W. *J. Am. Chem. Soc.* **1981**, *103*, 3597−3599. (f) Besecker, C. J.; Klemperer, W. G.; Day, V. W. *J. Am. Chem. Soc.* **1982**, *104*, 6158−6159. (g) Besecker, C. J.; Day, V. W.; Klemperer, W. G.; Thompson, M. R. *J. Am. Chem. Soc.* **1984**, *106*, 4125−4136. (h) Day, V. W.; Klemperer, W. G.; Maltbie, D. J. *Organometallics* **1985**, *4*, 104. (i) Besecker, C. J.; Day, V. W.; Klemperer, W. G.; Thompson, M. R. *Inorg. Chem.* **1985**, *24*, 44. (j) Day, V. W.; Klemperer, W. G.; Schwartz, C. *J. Am. Chem. Soc.* **1987**, *109*, 6030−6044. (k) Day, V. W.; Klemperer, W. G.; Maltbie, D. J. *J. Am. Chem. Soc.* **1987**, *109*, 2991. (l) Day, V. W.; Klemperer, W. G.; Lockledge, S. P.; Main, D. J. *J. Am. Chem. Soc.* **1990**, *112*, 2031. (m) Day, V. W.; Klemperer, W. G.; Main, D. J. *Inorg. Chem.* **1990**, *29*, 2345−2355. (n) Day, V. W.; Klemperer, W. G.; Main, D. J. *Inorg. Chem.* **1990**, *29*, 2355−2360.

(10) Tourné, C. *C. R. Acad. Sci. Ser. C.* **1968**, *226*, 702−704. Ho, R. K. C.; Klemperer, W. G. *J. Am. Chem. Soc.* **1978**, *100*, 6772−6774. Knoth, W. H.; Domaille, P. J.; Roe, D. C. *Inorg. Chem.* **1983**, *22*, 198−201. Domaille, P. J.; Knoth, W. H. *Inorg. Chem.* **1983**, *22*, 818−822. Maksimov, G. M.; Kuznetsova, L. I.; Matveev, K. I.; Maksimovskaya, R. I. *Koord. Khim.* **1985**, *11*, 1353−1357. Maksimov, G. M.; Kustova, G. N.; Matveev, K. I.; Lazarenko, T. P. *Koord. Khim.* **1989**, *15*, 788−796. Keana, J. F. W.; Ogan, M. D. *J. Am. Chem. Soc.* **1986**, *108*, 7951−7957. Lin, Y.; Weakley, T. J. R.; Rapko, B.; Finke, R. G. *Inorg. Chem.* **1993**, *32*, 5095−5101. Yamase, T.; Ozeki, T.; Sakamoto, H.; Nishiya, S.; Yamamoto, A. *Bull. Chem. Soc. Jpn.* **1993**, *66*, 103−108. Chen, Y. G.; Liu, J. F. *Polyhedron* **1996**, *15*, 3433−3436. Crano, N. J.; Chambers, R. C.; Lynch, V. M.; Fox, M. A. *J. Mol. Catal. A: Chem.* **1996**, *114*, 65−75. Detusheva, L. G.; Fedotov, M. A.; Kuznetsova, L. I.; Vlasov, A. A.; Likholobov, V. A. *Izv. Akad. Nauk, Ser. Khim.* **1997**, 914−920. Nomiya, K.; Arai, Y.; Shimizu, Y.; Takahashi, M.; Takayama, T.; Weiner, H.; Nagata, T.; Widegren, J. A.; Finke, R. G. *Inorg. Chim. Acta* **2000**, *300*−*302*, 285−304.

(11) Finke, R. G.; Rapko, B.; Weakley, T. J. R. *Inorg. Chem.* **1989**, *28*, 1573 and see Barnard, D. L.; Hill, C. L.; Cage, T.; Matheson, J. E.; Huffman, J. H.; Sidwell, R. W.; Otto, M. I.; Schinazi, R. F. *Intl. Antiviral News* **1995**, *3*, 159−161.

(12) The only Ta-containing HPAs we are aware of are reported in Torchenkova, E. A.; Nguyen Dieu; Kazanskii, L. P.; Spitsyn, V. I. *Izv. Akad. Nauk. SSSR, Ser. Khim.* **1973**, 734. Radkov, E.; Beer, R. H. *Polyhedron* **1995**, *14*, 2139. Radkov, E.; Lu, Y.-J.; Beer, R. H. *Inorg. Chem.* **1996**, *35*, 551−552.

(13) Wassermann, K.; Lunk, H.-J.; Palm, R.; Fuchs, J. *Acta Crystallogr.* **1994**, *C50*, 348. Wassermann, K.; Palm, R.; Lunk, H.-J.; Fuchs, J.; Steinfeld, N.; Stösser, R. *Inorg. Chem.* **1995**, *34*, 5029−5036. Wassermann, K.; Lunk, H.-J.; Palm, R.; Fuchs, J.; Steinfeld, N.; Stösser, R.; Pope, M. T. *Inorg. Chem.* **1996**, *35*, 3273−3279.

(14) The first lanthanide complex of a lacunary Wells−Dawson anion was reported by (a) Peacock, R. D.; Weakley, T. J. R. *J. Chem. Soc. A* **1971**, 1836. See more recent work of (b) Knoth, W. H.; Domaille, P. J.; Harlow, R. L. *Inorg. Chem.* **1986**, *25*, 1577−1584. (c) Bartis, J.; Dankova, M.; Lessmann, J. J.; Luo, Q.-H.; Horrocks, W. D., Jr.; Francesconi, L. C. *Inorg. Chem.* **1999**, *38*, 1042−1053. (d) Luo, Q.-H.; Howell, R. C.; Dankova, M.; Bartis, J.; Williams, C. W.; Horrocks, W. D., Jr.; Young, V. G., Jr.; Rheingold, A. L.; Francesconi, L. C.; Antonio, M. R. *Inorg. Chem.* **2001**, *40*, 1894−1901 and references therein.

(15) Knoth, W. H.; Domaille, P. J.; Roe, D. C. *Inorg. Chem.* **1983**, *22*, 198−201. Domaille, P. J.; Knoth, W. H. *Inorg. Chem.* **1983**, *22*, 818−822. Liu, J.; Ortega, F.; Sethuraman, F.; Katsoulis, D. E.; Costello, C. E.; Pope, M. T. *J. Chem. Soc., Dalton Trans.* **1992**, 1901. Xin, F.; Pope, M. T.; Long, G. J.; Russo, U. *Inorg. Chem.* **1996**, *35*, 1207−1213. Cowan, J. J.; Bailey, A. J.; Haintz, R. A.; Do, B. T.; Hardcastle, K, I.; Hill, C. L.; Weinstock, I. A. *Inorg. Chem.* **2001**, *40*, 6666−6675.

(16) (a) Weakley, T. J. R.; Evans, H. T.; Showell, J. S.; Tourné, C. M.; Tourné, G. F. *J. Chem. Soc., Chem. Commun.* **1973**, 139. (b) Finke, R. G.; Droege, M.; Hutchinson, J. R.; Gansow, O. *J. Am. Chem. Soc.* **1981**, *103*, 1587−1589. (c) Finke, R. G.; Droege, M. *Inorg. Chem.* **1983**, *22*, 1006−1008. (d) Evans, H. T.; Tourné, C. M.; Tourné, G. F.; Weakley, T. J. R. *J. Chem. Soc., Dalton Trans.* **1986**, 2699−2705. (e) Finke, R. G.; Droege, M. W.; Domaille, P. J. *Inorg. Chem.* **1987**, *26*, 3886−3896. (f) Weakley, T. J. R.; Finke, R. G. *Inorg. Chem.* **1990**, *29*, 1235−1241. (g) Gómez-García, C. J.; Coronado, E.; Borrás-Almenar, J. J. *Inorg. Chem.* **1992**, *31*, 1667. (h) Casañ-Pastor, N.; Bas-Serra, J.; Coronado, E.; Pourroy, G.; Baker, L. C. W. *J. Am. Chem. Soc.* **1992**, *114*, 10380. (i) Gómez-García, C. J.; Coronado, E.; Gómez-Romero, P.; Casañ-Pastor, N. *Inorg. Chem.* **1993**, *32*, 3378. (j) Gómez-García, C. J.; Borrás-Almenar, J. J.; Coronado, E.; Ouahab, L. *Inorg. Chem.* **1994**, *33*, 4016−4022. (k) Zhang, X.; Jameson, G. B.; O'Connor, C. J.; Pope, M. T. *Polyhedron* **1996**, *15*, 917. (l) Zhang, X.; Chen, Q.; Duncan, D. C.; Campana, C.; Hill, C. L. *Inorg. Chem.* **1997**, *36*, 4208. (m) Zhang, X.; Chen, Q.; Duncan, D. C.; Lachicotte, R. J.; Hill, C. L. *Inorg. Chem.* **1997**, *36*, 4381. (n) Clemente-Juan, J. M.; Coronado, E.; Galán-Mascarós, J. R. Gómez-García, C. J. *Inorg. Chem.* **1999**, *38*, 55 (o) Andres, H.; Clemente-Juan, J. M.; Basler, R.; Aebersold, M.; Güdel, H.-U.; Borrás-Almenar, J. J.; Gaita, A.; Coronado, E.; Büttner, H.; Janssen, S. *Inorg. Chem.* **2001**, *40*, 1943−1950.

(17) Anderson, T. M.; Hardcastle, K. I.; Okun, N.; Hill, C. L. *Inorg. Chem.* **2001**, *40*, 6418−6425.

(18) Maestre, J. M.; López, X.; Bo, C.; Casañ-Pastor, N.; Poblet, J. M. *J. Am. Chem. Soc.* **2001**, *123*, 3749−3758.

(19) López, X.; Maestre, J. M.; Bo, C.; Poblet, J. M. *J. Am. Chem. Soc.* **2001**, *123*, 9571−9576.

(20) Duclusaud, H.; Borshch, S. A. *Inorg. Chem.* **1999**, *38*, 3489−3493.

(21) Duclusaud, H.; Borshch, S. A. *J. Am. Chem. Soc.* **2001**, *123*, 2825−2829.

(22) Synthetic and organometallic-related work developed in (a) Finke, R. G.; Droege, M. W. *J. Am. Chem. Soc.* **1984**, *106*, 7274−7277. (b) Domaille, P. J. *J. Am. Chem. Soc.* **1984**, *103*, 7677−7687. (c) Domaille, P. J.; Watunya, G. *Inorg. Chem.* **1986**, *25*, 1239−1242. (d) Finke, R. G.; Rapko, B.; Saxton, R. J.; Domaille, P. J. *J. Am. Chem. Soc.* **1986**, *108*, 2947−2960. (e) Edlund, D. J.; Saxton, R. J.; Lyon, D. K.; Finke, R. G. *Organometallics* **1988**, *7*, 1692−1704. (f) Trovarelli, A.; Finke, R. G. *Inorg. Chem.* **1993**, *32*, 6034−6039. (g) Lin, Y.; Nomiya, K.; Finke, R. G. *Inorg. Chem.* **1993**, *32*, 6040−6045. (h) Nomiya, K.; Kaneko, M.; Kasuga, N. C.; Finke, R. G.; Pohl, M. *Inorg. Chem.* **1994**, *33*, 1469−1472. (i) Rapko, B. M.; Pohl, M.; Finke, R. G. *Inorg. Chem.* **1994**, *33*, 3625−3634. (j) Lin, Y.; Finke, R. G. *Inorg. Chem.* **1994**, *33*, 4891−4910. (k) Pohl, M.; Lin, Y.; Weakley, T. J. R.; Nomiya, K.; Kaneko, M.; Weiner, H.; Finke, R. G. *Inorg. Chem.* **1995**, *34*, 767−777. (l) Pohl, M.; Lyon, D. K.; Mizuno, N.; Nomiya, K.; Finke, R. G. *Inorg. Chem.* **1995**, *34*, 1413−1429. (m) Weiner, H.; Aiken, J. D., III; Finke, R. G. *Inorg. Chem.* **1996**, *35*, 7905−7913. (n) Weiner, H.; Hayashi, Y.; Finke, R. G. *Inorg. Chem.* **1999**, *38*, 2579−2591.

(23) Most of the electrochemical work in mixed-addenda Wells−Dawson compounds has been developed by Contant, Nadjo, and co-workers. Some recent publications are (a) Keita, B.; Belhouari, A.; Nadjo, L.; Contant, R. *J. Electroanal. Chem.* **1998**, *442*, 49−57. (b) Keita, B.; Girard, F.; Nadjo, L.; Contant, R.; Canny, J.; Richet, M. *J. Electroanal. Chem.* **1999**, *478*, 76−82. (c) Keita, B.; Lu, Y. W.; Nadjo, L.; Contant, R.; Abbessi, M.; Canny, J.; Richet, M. *J. Electroanal. Chem.* **1999**, *477*, 146−157. (d) Contant, R.; Abbessi, M.; Canny, J.; Richet, M.; Keita, B.; Belhouari, A.; Nadjo, L. *Eur. J. Inorg. Chem.* **2000**, 567−574. (e) Keita, B.; Lu, Y. W.; Nadjo, L.; Contant, R. *Eur. J. Inorg. Chem.* **2000**, 2463−2471.

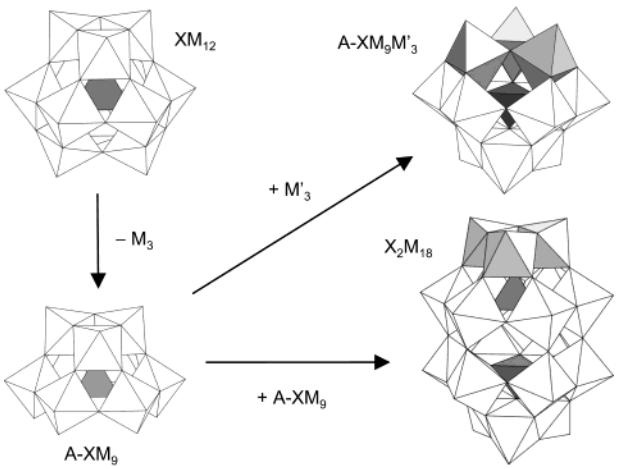

Figure 1. Polyhedral representation of the α-XM_{12} Keggin anion, the A-XM_9 lacunary anion derived by removing three corner-sharing octahedra, and the mixed-addenda A-$XM_9M'_3$ and the Wells−Dawson structure P_2M_{18} formed by adding an M'_3 or another A-XM_9 unit, respectively.

M_3O_{15} corner-sharing triads (*A-triads*). Figure 1 shows, in polyhedral representation, the pattern of three neighboring octahedra that are removed from the Keggin framework to give the lacunary A-form. Of the lacunary XM_9 units, the anions that contain A-fragments are the most frequent, although many aggregates of the B-XM_9 precursor are also known.[24] All the structures reported in the present work are formal derivatives of the Keggin anion: the A-$[SiW_9M_3O_{40}]^{n-}$ species maintain their shape after the substitution, and the W−D structures are an assembly of two A-XM_9O_{34} units.

Theoretical Details

The calculations were carried out using the DFT methodology with the ADF2000 program.[25] The local density approximation (LDA) characterized by the electron-gas exchange together with the Vosko−Wilk−Nusair[26] (VWN) parametrization for correlation were used. Gradients were corrected by means of the Becke[27] and Perdew[28] nonlocal corrections to the exchange and correlation energy, respectively. Triple-ζ plus polarization Slater basis sets were used to describe the valence electrons of main group atoms, (Si, P) whereas for transition-metal atoms a frozen core composed of 1s to 2p shells for vanadium, 1s to 3spd shells for niobium and molybdenum, as well as 1s to 4spd shells for the sixth period element, tungsten, were described by means of single Slater functions. *n*s and *n*p electrons were described by double-ζ Slater functions, *n*d and $(n + 1)$s by triple-ζ functions, and $(n + 1)$p by a single orbital.[29] The Pauli formalism with corrected core potentials was used to make quasirelativistic corrections for the core electrons. The quasirelativistic frozen core shells were generated using the auxiliary program DIRAC.[25] Open shell electronic configurations were computed with the unrestricted methodology. The solvent effects were included by means of the COSMO[30] software, included in the ADF2000 package. The geometries of the Keggin and Wells−Dawson anions were fully optimized for each state.

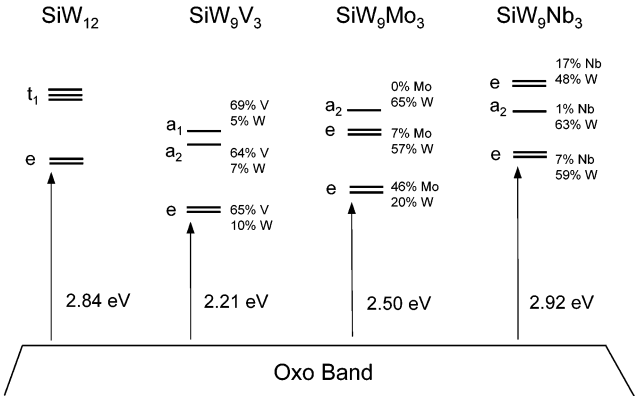

Figure 2. Diagram of the molecular orbitals for the α-$[SiW_{12}O_{40}]^{4-}$ and the trisubstituted A-α-$[SiW_9M_3O_{40}]^{n-}$ anions, with M = V, Mo, and Nb, from left to right.

Results and Discussion

Addenda-Substituted Keggin Anions. The electronic structure of the fully oxidized XM_{12} anions is quite simple and can be described in terms of the energy levels and shape of the molecular orbitals (MOs). Two sets of orbitals are easily identifiable in Keggin clusters without paramagnetic ions: a set of doubly occupied MOs, delocalized over the oxo ligands, and a set of unoccupied d-like addenda orbitals that conform the metallic band. In this band, the lowest orbitals are symmetry-adapted combinations of d_{xy}-like orbitals with some antibonding participation of oxygen orbitals. The d_{xz}- and d_{yz}-type orbitals are higher in energy since the shorter terminal bonds destabilize them.[18] For the tungsto-derivatives A-α-SiW_9M_3, with M = Mo, V, and Nb, full geometry optimizations were carried out under C_{3v} symmetry constraints. In general, present DFT calculations reproduce very well the geometry of the heteropolyanions with the exception of the metal-terminal oxygen bond lengths that are computed systematically longer than the experimental ones. The deviations are on average 0.04 Å and seem to depend on the net charge in the internal tetrahedron.[18] The empty set of d-tungsten orbitals appears, after the metallic substitution, as a mixture of W and M orbitals. The order and composition of the molecular orbitals depend heavily on M. There is no doubt that the redox properties of the substituted cluster will depend on the nature and energy of the lowest unoccupied orbitals. In the dodecatungstates, the HOMO−LUMO (H−L) gap was computed to be ∼2.8 eV (Figure 2). This energy decreases to ∼2 eV for molybdates. The lower H−L gap in molybdates means that they are, in general, more easily reduced. Hence, for instance, $SiMo_{12}$ and $GeMo_{12}$ are more powerful oxidizing agents than the corresponding tungstates by ∼0.5 V.[31] The other fundamental variable that plays an essential role in the oxidant power is the total negative charge of the anion. Pope and Varga

(24) (a) Hervé, G.; Tézé, A. *Inorg. Chem.* **1977**, *16*, 2115. (b) Massart, R.; Contant, R.; Fruchart, J. M.; Ciabrini, J. P.; Fournier, M. *Inorg. Chem.* **1977**, *16*, 2916. (c) Jeannin, Y.; Martin-Frère, J. *J. Am. Chem. Soc.* **1981**, *103*, 1664−1667. (d) Martin-Frère, J.; Jeannin, Y. *Inorg. Chem.* **1984**, *23*, 3394−3398. (e) Weakley, T. R. J. *J. Chem. Soc., Chem. Commun.* **1984**, 1406. (f) Kortz, U.; Tézé, A.; Hervé, G. *Inorg. Chem.* **1999**, *38*, 2038−2042. (g) References 16a−b,d−g, 22b.
(25) *ADF 2000.01*; Department of Theoretical Chemistry, Vrije Universiteit: Amsterdam. Baerends, E. J.; Ellis, D. E.; Ros, P. *Chem. Phys.* **1973**, *2*, 41−51. Versluis, L.; Ziegler, T. *J. Chem. Phys.* **1988**, *88*, 322−328. Te Velde, G.; Baerends, E. J. *J. Comput. Phys.* **1992**, *99*, 84−98. Fonseca Guerra, C.; Snijders, J. G.; Te Velde, G.; Baerends, E. J. *Theor. Chem. Acc.* **1998**, *99*, 391−403.
(26) Vosko, S. H.; Wilk, L.; Nusair, M. *Can. J. Phys.* **1980**, *58*, 1200.
(27) Becke, A. D. *J. Chem. Phys.* **1986,** *84*, 4524; *Phys. Rev.* **1988**, *A38*, 3098.
(28) Perdew, J. P. *Phys. Rev.* **1986**, *84*, 4524; **1986**, *A34*, 7406.
(29) Snijders, J. G.; Baerends, E. J.; Vernooijs, P. *At. Nucl. Data Tables* **1982**, *26*, 483. Vernooijs, P.; Snijders, J. G.; Baerends, E. J. *Slater type basis functions for the whole periodic system*; Internal Report, Free University of Amsterdam: Amsterdam, The Netherlands, 1981.
(30) Pye, C. C.; Ziegler, T. *Theor. Chem. Acc.* **1999**, *101*, 396.

rationalized the first cathodic potential dependence with the negative charge for Keggin anions.[32] The substitution of three tungsten ions by three molybdenum ions modifies the relative energy of the LUMO from 2.8 eV in the dodecatungstate to 2.5 eV in A-α-SiW_9Mo_3. In the tungstomolybdate, the LUMO is a degenerate orbital of e symmetry with a larger participation of d-molybdenum orbitals. Since the total charge of the anion does not change, the simple substitution of tungsten by molybdenum increases the oxidizing power of the anion. In particular, present DFT calculations indicate that the mono-reduction of SiW_9Mo_3 is ∼0.4 eV more favorable than that of SiW_{12}, a value comparable to the previously reported 0.54 V obtained experimentally.[33]

The group 5 derivative, A-α-SiW_9V_3, has an H−L gap of 2.21 eV, an even lower energy than that computed for A-α-SiW_9Mo_3. The LUMO in the vanadium derivative, which is a degenerate orbital of e symmetry, and the LUMO+1, which appears ∼2.9 eV from the HOMO, are d_{xy}-orbitals essentially localized on the vanadium centers. This means that the vanadotungstate will preferentially be reduced in the vanadium centers, as electrochemical studies by Hervé and co-workers have demonstrated.[34,35] On the other hand, the analogous niobium derivative has an H−L gap of 2.92 eV, somewhat larger than the single addenda dodecatungstate. This behavior combined with the higher negative charge in the substituted derivative means that the substitution of W by Nb always decreases the oxidizing power of the anion.

The relative energy and composition of the LUMO correlate quite well with the electron affinity of each *isolated* M^{n+} ion that is in the order $Mo^{6+} > V^{5+} > W^{6+} \gg Nb^{5+}$. Although the first ionization potential of W is greater than that of Mo, there is an inversion in the subsequent ionization energies and the 6th ionization potential is higher for Mo. +68.10 eV (Mo) and +63.95 eV (W) are the 6th ionization potentials computed at the present level of theory. In contrast, Nb systematically shows a greater predisposition than V to lose its electrons. In agreement with these ionization energies, present DFT calculations gave the following LUMO compositions: for the tungsten-niobate, only 7% of Nb and 59% of W contribution. When M = Mo, the sharing of the LUMO is 46/20% for Mo/W and, finally, the LUMO has the largest heteroatom participation, 65%, for SiW_9V_3. The tungsten contribution is 10%. This mixed cluster has the lowest H−L gap. Unrestricted calculations of single-reduced Keggin anions were performed to check predictions made by orbital analysis. Jahn−Teller effects might take place in monoreduced species since a degenerate *e* orbital is populated with one electron. Nevertheless, previous calculations on single addenda Keggin anions[19] showed that the stabilization due to the Jahn−Teller effect is very small, and it has not been considered here. Spin polarizations given in Table 1 reinforce the qualitative predictions based on the molecular orbitals of the oxidized species, which suggest that the additional electron in the monoreduced species A-α-SiW_9V_3 is delocalized among the three vanadium centers (0.35 spin alpha electrons per V). Some extra polarization in the molecule yields a population of 0.012 spin alpha electrons per W. In the analogous molybdate, 70% of the additional electron is distributed among the three Mo centers. Finally, when the substituting addenda is a Nb^{5+}, the orbitals of the heteroatom do not participate in the LUMO and the spin density is localized in the W centers in 87%. Although the ionization energies of isolated metal ions would suggest that the reduction of mixed molybdovanadates would take place at the molybdenum centers, the extra electron mostly goes to a vanadium atom.[18,34] In Figure 2, the V orbital is the lowest of the four LUMO. The particular behavior of the Mo^{6+} and V^{5+} pair arises from the different electronic population of d orbitals in fully oxidized clusters, which is larger for Mo atoms.

Table 1. Spin Polarizations (α−β Electrons) for Several Single-Reduced A-α-$[SiW_9M_3O_{40}]^{n-}$ Anions

	spin polarization	
anion	W	M
A-$[SiW_9Mo_3O_{40}]^{5-}$	0.20	0.72
A-$[SiW_9V_3O_{40}]^{8-}$	0.15	1.04
A-$[SiW_9Nb_3O_{40}]^{8-}$	0.87	0.13

Electronic Structure of Wells−Dawson Anions. ESR and electrochemical studies[36] have shown that W−D anions are chemically different from Keggin species because of their structural differences. Hence, whereas all metals are equivalent in the α-Keggin anion, a clear distinction can be made between polar (*cap* regions) and equatorial octahedrons (*belts*) in the W−D framework. The equatorial M_{12} array is formed via alternative corner- and edge-sharing of the MO_6 units, as can be deduced from Figure 1. They are also linked to polar octahedra by a single corner per MO_6 group. This makes W−D molecules different from the Keggin anions, in which every octahedron shares two edges with neighboring MO_6 units. Special attention should be paid to the M−O−M angle of the corner-sharing octahedra in the equatorial zone, which was computed to be 163° in both P_2W_{18} and P_2Mo_{18}; the experimentally measured value is 162°.[37] The corresponding M−O−M angle in the *cap* is close to 125°. The presence of almost linear M−O−M angles linking the two halves of the anion implies these two adjacent metals to be separated by 3.7−3.8 Å, while in a PM_9 moiety the distance between two neighboring metals is ∼3.4 Å. We will show that this structural characteristic determines the electronic properties and, therefore, the redox chemistry of W−D molecules.[38] The other structural parameters are much less important: all the M=O (terminal) bond lengths were computed to be ∼1.74 Å, a value that is very similar to the M=O distance found for XM_{12} structures[18,19] and is 0.05 Å longer than the experimental distance.[5,37] The M−O (bridge) distances are also similar to those found in Keggin anions. They are about 1.90−1.94 Å in the tungstate. The deviations in the

(31) Hervé, G. *Ann. Chim. (Paris)* **1971**, *6*, 219; **1971**, *6*, 287. Launay, J. P.; Massart, R.; Souchay, P. *J. Less-Common Met.* **1974**, *36*, 139. Altenan, J. J.; Pope, M. T.; Prados, R. A.; So, H. *Inorg. Chem.* **1975**, *14*, 417; Maeda, K.; Katano, H.; Osakai, T.; Himeno, S. *J. Electroanal. Chem.* **1995**, *389*, 167.
(32) Pope, M. T.; Varga, G. M. *Inorg. Chem.* **1966**, *5*, 1249−1254.
(33) Souchay, R.; Hervé, G. *C. R. Acad. Sci., Ser. C.* **1965**, *261*, 2486. Contant, R.; Fruchart, J. M.; Hervé, G.; Tézé, A. *C. R. Acad. Sci., Ser. C.* **1974**, *278*, 199.
(34) Cadot, E.; Fournier, M.; Tézé, A.; Hervé, G. *Inorg. Chem.* **1996**, *35*, 282−288.
(35) Mossoba, M. M.; O'Connor, C. J.; Pope, M. T.; Sinn, E.; Hervé, G.; Tézé, A. *J. Am. Chem. Soc.* **1980**, *22*, 6864−6866.
(36) See ref 38b for the first assignment proposed for cathodic waves in the reduction of 2:18 anions.
(37) Strandberg, R. *Acta Chem. Scand., Ser. A.* **1975**, *29*, 350.
(38) (a) Pope, M. T.; Papaconstantinou, E. *Inorg. Chem.* **1967**, *6*, 1147. (b) Varga, G. M.; Papaconstantinou, E.; Pope, M. T. *Inorg. Chem.* **1970**, *9*, 662. (c) Papaconstantinou, E.; Pope, M. T. *Inorg. Chem.* **1970**, *9*, 667.

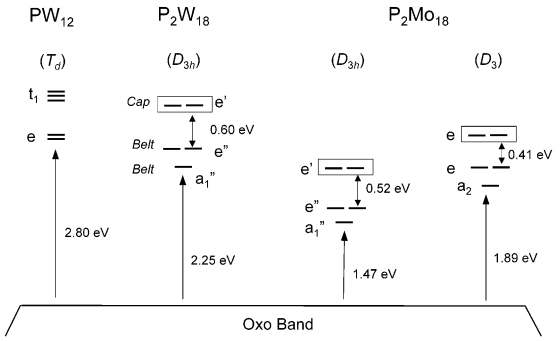

Figure 3. Molecular orbitals scheme for the α-PW_{12} anion and the single-addenda Wells−Dawson heteropolyanions with M = W and Mo. In the latter case, we show the orbitals associated to the D_{3h} and D_3 structures. The orbitals in frames are those localized on the polar triads of the corresponding Wells−Dawson anions.

Table 2. Percentile Contributions of Belt and Cap Metal Centers to the LUMO, LUMO+1, and LUMO+2 for Several Wells−Dawson Anions

anion	sym	belt	cap	belt	cap	belt	cap
		a_1''		e''		e'	
P_2W_{18}	D_{3h}	70	0.5	61	10	20	48
P_2Mo_{18}	D_{3h}	62	1	54	9	22	40
		e		a_2		e	
$P_2W_{15}V_3$	C_{3v}	13	60	65	0	55	10
$P_2Mo_{15}V_3$	C_{3v}	36	33	59	0	39	26
$P_2W_{15}Mo_3$	C_{3v}	70	2	55	15	49	19

terminal bonds should not alter the reduction properties discussed in the present work since they essentially would affect the d_{xz}- and d_{yz}- type orbitals that are not the lowest ones.

W−D anions present the typical MO arrangement of HPAs, where the oxo band and the empty set of d_{xy} metal orbitals are perfectly separated. The redox properties of a POM are closely related to the relative energy and composition of the lowest unoccupied orbitals. In an α-Keggin anion, the twelve metals are equivalent and, therefore, they all have the same probability of trapping the additional electron after the cluster has been reduced. In an α-Keggin, the formal substitution of three octahedrons by another PM_9 unit breaks the equivalence of all metals and a direct consequence is that the metallic orbitals in the W−D and Keggin anions are slightly different. Figure 3 contains an energy diagram for the lowest unoccupied orbitals of 1:12 and 2:18 tungstates and molybdates and Table 2 gives percentile metal contributions to the LUMO, LUMO+1, and LUMO+2 for all the W−D anions studied. All these unoccupied orbitals, like in the Keggin anions, are formally symmetry-adapted d_{xy}-tungsten orbitals with some antibonding participation of the oxygen orbitals. Under the constraints of the D_{3h} point group, their symmetries are a_1'', e'', and e', respectively. The contribution of cap and belt metals to these three orbitals is unequal; the d_{xy}-orbitals centered on the belt metals are the major contributors to the LUMO and LUMO+1. When the energy of the orbital increases, the participation of the cap-centered atomic orbitals also increases (from ∼1% in the LUMO to ∼48% in the LUMO+2 in the tungstate and to ∼40% in the molybdate). A 3D representation of the a_1'' orbital (Figure 4) shows that the LUMO is only localized over the *belt* tungstens. This orbital appears at 2.25 eV above the occupied oxo band and 0.55 eV lower than the degenerate LUMO of e symmetry in the PW_{12} anion of T_d symmetry. The metallic orbitals in PW_{12} and P_2W_{18} have an antibonding character between the metal and oxygen

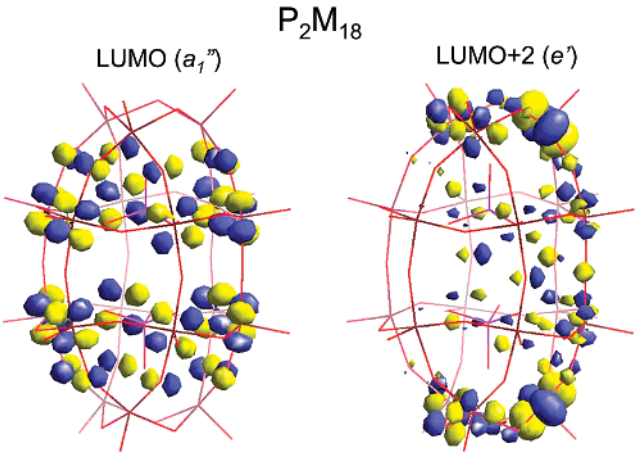

Figure 4. 3D representation of the LUMO (a_1'') and LUMO+2 (e', one component) of P_2W_{18}. Only the frontal part of the molecule is represented for clarity in a_1''.

orbitals but also between two adjacent metals. The M−M antibonding interaction is lower when the two adjacent metals belong to two different PW_9 moieties (the metal−metal distances are longer), and therefore the d_{xy}-type orbitals delocalized among the equatorial tungstens have lower energies than the corresponding orbitals in the Keggin structure. Exactly the same behavior occurs in the molybdate. 1.47 eV is the relative energy of the LUMO in the D_{3h} P_2Mo_{18} anion, an energy that represents a decrease of 0.56 eV with respect to the H−L gap in PMo_{12}. The α-P_2Mo_{18} anion is very interesting since it has been characterized as a chiral structure of D_3 symmetry.[5b,37,39,40] The molybdenum atoms are displaced within their respective MoO_6 octahedra, which gives rise to loops of alternatively *short* (∼1.80 Å) and *long* (∼2.05 Å) Mo−O−Mo bonds.[39b] Calculations carried out with the D_3 symmetry reproduced very well the experimental structure with short and long Mo−O−Mo bonds (1.82 and 2.12 Å, respectively). All Mo═O bond lengths were found to be ∼1.74 Å, the same distance computed for terminal bonds in the homologous tungstate. The lowering of the symmetry from D_{3h} to D_3 is accompanied by a considerable stabilization of 0.32 eV (>7 kcal mol^{-1}) and an enlargement of the H−L gap to 1.89 eV, a value that is quite close to the energy gap of 2.03 eV found for PMo_{12}. In general, the transformation of a PM_{12} into a P_2M_{18} decreases the H−L gap more in tungstates than in molybdates (Figure 3).

The redox properties of heteropolyanions are closely related to the energy and composition of the LUMO. According to the orbital diagram in Figure 3, the first reduction in the W−D anions should take place in the belt region. Calculations conducted on the reduced structures confirmed this hypothesis and the ground state for the single-reduced P_2W_{18} is a $^2A_1''$ with 98% of the spin density localized over the belt metals (Table 3). The first excited state ($^2E''$) has the spin density essentially localized over the belt metal centers (87%) and lies at 0.30 eV above the ground state. The reduction in the cap sites involves the addition of one electron to the LUMO+2 (e') and the associated state $^2E'$ is 0.84 eV higher in energy than the ground state. The spin polarization for $^2E'$ is 0.69 alpha

(39) (a) Prados, R. A.; Pope, M. T. *Inorg. Chem.* **1976**, *15*, 2547−2553. (b) Garvey, J. F.; Pope, M. T. *Inorg. Chem.* **1978**, *17*, 1115−1118.
(40) Harmalker, S. P.; Leparulo, M. A.; Pope, M. T. *J. Am. Chem. Soc.* **1983**, *105*, 4286−4292.

Table 3. Spin Densities on Belt and Cap Metal Centers ($\alpha-\beta$) and Relative Energies (in eV) for the First Three Lowest States in Several Single-Reduced Wells−Dawson Anions

	sym	($\alpha-\beta$)		energy	($\alpha-\beta$)		energy	($\alpha-\beta$)		energy
		$^2A_1$			$^2E''$			$^2E'$		
		belt	cap		belt	cap		belt	cap	
P_2W_{18}	D_{3h}	0.98	−0.03	0.00	0.87	0.13	0.30	0.26	0.69	0.84
P_2Mo_{18}	D_{3h}	0.89	−0.05	0.00	0.83	0.14	0.20	0.27	0.66	0.69
		^2E			$^2A_2$					
$P_2W_{15}V_3$	C_{3v}	0.18	1.00	0.00	0.88	−0.011	0.33			
$P_2Mo_{15}V_3$	C_{3v}	0.44	0.55	0.00	0.81	−0.020	0.18			
$P_2W_{15}Mo_3$	C_{3v}	0.34	0.61	0.00	0.98	−0.03	−0.018			

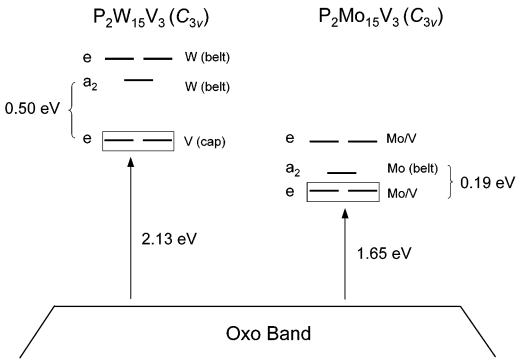

Figure 5. Molecular orbital diagram for the cap trisubstituted $P_2W_{15}V_3$ and $P_2Mo_{15}V_3$ heteropolyanions.

electrons delocalized among the six cap tungsten atoms and 0.26 e among the twelve belt centers. For the analogous molybdate structure, the energy associated to the belt ($^2A_1''$) and cap ($^2E'$) reductions differs by 0.69 eV for the D_{3h} isomer (exactly the energy gap between the LUMO and the LUMO+2). In the D_3 form, the separation between these MOs is the same, which suggests that the energy difference between both site reductions should be very close to the value obtained for the D_{3h} form. All these results fully agree with the experimental data of Pope[38b] and Contant[23] who demonstrated that equatorial sites are more easily reduced than polar sites.

Effect of the Chemical Substitution on the Redox Properties of the Wells−Dawson Anions. If we wish to invert the traditional belt/site reduction order, a more electronegative ion must be inserted in the polar region. $P_2W_{15}V_3$ and $P_2Mo_{15}V_3$ are suitable anions for illustrating this phenomenon. In these two clusters, the three vanadium atoms occupy the three cap sites of one PM_9 moiety. Calculations were carried out using the restrictions of the C_{3v} symmetry group. Now, two factors—the *most favorable belt position* and the *higher electronegativity* of the V^V ion—strongly compete to capture the additional electron. When three vanadiums replace three cap tungstens in P_2W_{18}, there is an inversion in the order of belt/cap d_{xy}-like orbitals. The degenerate orbital of e symmetry (e′ in the unsubstituted species), mainly centered on the cap region, turns out to be the LUMO in the substituted molecule and appears well separated (0.50 eV) from the next two orbitals of a_2 and e symmetries, which are basically d−W (belt) orbitals (Figure 5). According to this orbital ordering, the first reduction occurs in vanadium cap orbitals and the energy difference between the two site reductions ($^2E - {}^2A_2$) was 0.33 eV. The spin polarization for the ^2E ground state of $P_2W_{15}V_3$ 1e confirms that the additional electron is essentially located on the vanadium centers (Table 3). We did not study the substitution in the equatorial positions, but in this case the lowest unoccupied orbital should be a vanadium orbital with a larger energy gap between the LUMO and LUMO+1. Thus, the first reduction should take place in the belt sites and the difference between the belt and cap reduction should be greater than in the cap substitution. All these results totally agree with the studies of Pope and co-workers,[37] who used cyclic voltammograms to find that the most positive cathodic peak for $P_2W_{17}V$ appears when the vanadium occupies a belt site. The ESR spectra of anions substituted solely at the polar sites, $P_2V^{IV}V^VW_{16}$ and $P_2V^{IV}V_2VW_{15}$, show that the metallic electron is effectively trapped by the vanadium centers.[41]

In the analogous vanadomolybdate heteropolyanion, there is considerable competition between vanadium and molybdenum orbitals. As Table 2 shows, the LUMO of e symmetry in $P_2Mo_{15}V_3$ is not localized on one of the regions of the molecule and the participation of belt Mo (36%) and cap V (33%) orbitals is similar. The next metallic orbital of a_2 symmetry is only separated from the LUMO by 0.19 eV and is basically a belt orbital (59%). This competition between Mo and V orbitals yields a spin density distribution in the reduced complex of 0.55 e for cap V atoms and 0.44 e for belt Mo atoms. The energy difference between the two states ^2E and $^2A_2$ was computed to be only 0.18 eV. This competition is still more important in $P_2W_{15}Mo_3$ since those two states associated to the first reduction in cap (^2E) and belt ($^2A_2$) sites were found degenerate, a result that does not fully match with the fact that the first reductions in $P_2W_{15}Mo_3$ are restricted to the Mo centers.[42,43] Although the origin of this discrepancy is unclear, we believe that present DFT calculations probably exaggerate the energy gap between cap and belt reductions for a given metal. The localization/delocalization of the orbitals may depend on the method applied. In general, Hartree−Fock techniques tend to overlocalize the electrons whereas the methods based on density functionals overestimate the delocalization.[44] In an independent study, Jean, Nadjo, and co-workers have performed a qualitative analysis of W−D type heteropolyanions on the basis of Extended Hückel calculations, also concluding that the change of the reduction site upon substitution in the cap region by a more electronegative metal center is consistent with the localization of the LUMO on the substituted center.[45]

Basicity of External Oxygen Sites in Mixed-Addenda Keggin Anions. The high basicity of the oxo ligands is another of the fundamental properties of POMs.[9a,g,j−k] In single-addenda Keggin anions, there are two different sites, the bridging OM_2 oxygen and the terminal OM oxygen. In fact, there are two distinct bridging oxygens but the differences between them are rather small. The substitution of a W or a Mo by another metal may modify the charge density throughout the POM and alter the relative basicity of the various sites in the molecule. In general, the basicity of the oxygen sites depends on the number of metals linked to the oxo ligand. Hence, for example, experimental[46] and theoretical[47] studies on the decavanadate

(41) Harmalker, S. P.; Pope, M. T. *J. Am. Chem. Soc.* **1981**, *103*, 7381−7383.
(42) Kozik, M.; Hammer, C. F.; Baker, L. C. W. *J. Am. Chem. Soc.* **1986**, *108*, 2748; **1986**, *108*, 7627.
(43) Kozik, M.; Baker, L. C. W. *J. Am. Chem. Soc.* **1990**, *112*, 7604.
(44) Picket, W. E. *Rev. Mod. Phys.* **1989**, *61*, 433. Illas, F.; Martin, R. *J. Chem. Phys.* **1998**, *108*, 2519. Martin, R.; Illas, F. *Phys. Rev. Lett.* **1997**, *79*, 1539.
(45) Keita, B.; Jean, Y.; Levy, B.; Nadjo, L.; Contant, R. *New J. Chem.*, in press.
(46) Day, V. W.; Klemperer, W. G.; Maltbie, D. J. *J. Am. Chem. Soc.* **1987**, *109*, 2991.

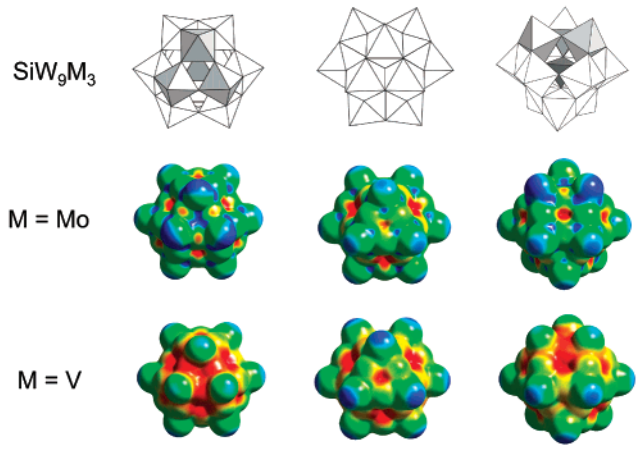

Figure 6. Molecular electrostatic potentials (MEPs) from three different viewpoints (see polyhedral representations) for the SiW_9M_3 derivatives with M = Mo and V. See text for further details.

anion $[V_{10}O_{28}]^{6-}$ showed that the oxygen bonded to three vanadiums is more basic than bridging oxygens and the terminal oxygens are the least basic sites. From the theoretical point of view, the topology of the molecular electrostatic potentials (MEP) proved to be very useful for detecting the most electrophilic regions of a POM. Electrophilic species will tend to minimize its potential energy by approaching as much as possible a minimum of the MEP distribution.

Figure 6 shows three views of the MEP distribution on a 3D surface for the mixed anions SiW_9M_3 (M = Mo and V). The color of the electronic density isosurface ($\rho = 0.017$ e/ua) is a function of the MEP value. In the figure, red identifies regions in which the electrostatic potential is negative (nucleophilic regions) and blue denotes positive or less negative electrostatic potential regions (electrophilic sites). When tungstens are substituted by molybdenums in SiW_{12}, the electronic reorganization is quite small and the basicity of the substituted anion is not very different from that of the single-addenda anion. Clearly, bridging oxygens are generally more basic than terminal oxygens in the MEP of SiW_9Mo_3 since the regions close to terminal OMo and OW oxygen sites (dark blue) are the least basic, and the accessible nucleophilic regions (red) are close to the bridging oxygens. In Figure 6, the red color is darker in the vicinity of the most internal regions dominated by the potential of the tetrahedral oxygens, the only oxo ligand bonded to four positive ions. This oxygen, however, is not easily accessible for a proton. A simple analysis of the MEP indicates that, on one hand, the bridging OMo_2 sites should be the most favorable for a protonation and, on the other, that the terminal OMo oxygen is not a good position for protonation. Calculating the structure of the corresponding protonated forms corroborated this hypothesis. Table 4 lists the values of the relative protonation energies for the six isomers H−OM_2, H−OM, H−OW_2-(2), H−OWM, and H−OW. The energy sequence matches the qualitative ideas that emanate from the MEP distribution analysis. The most stable protonated complex is the isomer in which the proton is attached to the bridging oxygen linked to two molybdenum ions. The next preferred site is OMoW with a relative energy of only 3.7 kcal mol^{-1}, and OW_2 is the least basic of the bridging oxygens and lies at 6.8 kcal mol^{-1}. The

Table 4. Relative Protonation Energies (in kcal mol^{-1}) for All the Distinct External Oxygens of A-α-$[SiW_9M_3O_{40}]^{n-}$, with M = Mo and V[a]

M	site	relative energy
Mo	OMo_2	−4.9
	OMoW	−1.2
	OW_2	0.0
	OW	+11.0
	OMo	+15.0
V	OV_2	−12.4
	OVW	−1.4
	OW_2	0.0
	OV	+5.6
	OW	+19.2

[a] For a better comparison between the two clusters, the zero-energy protonation site was arbitrarily chosen to be OW_2.

energies of H−OMo and H−OW isomers were computed to be 19.8 and 15.9 kcal mol^{-1} above the energy of H−OMo_2, respectively. These results are consistent with the acidity order of HPAs, for which tungstates are slightly more acidic than molybdates.[48]

Clearly, in the MEP distribution of the group 5 derivative SiW_9V_3 (Figure 6) the differences in proton affinity between the most basic and the least basic sites are larger than in W/Mo mixed anions. The blue color in the vicinity of terminal OW oxygens indicates that these sites should be the least basic. In contrast, the wide red area in the domains of OV_2 oxygens is a strong signal that these sites should have the largest proton affinity. Again, the calculations carried out on the protonated forms fully confirmed the predictions made from electrostatic potential maps since H−OV_2 is the most stable isomer for $HSiW_9V_3$. Our calculations suggest the following oxygen basicity scale in SiW_9V_3: OV_2 > OVW > OW_2 > OV > OW, the difference in the proton affinity between the most and least basic sites being ∼30 kcal mol^{-1}. This is ∼10 kcal mol^{-1} greater than in the tungstomolybdate anion.

A proton residing in a bridging oxygen OM'_2 with M′ = W, Mo, or V and on a terminal OM′ has energy differences, according to present DFT calculations, that range between 9 and 20 kcal mol^{-1}, a considerable amount of energy but significantly lower than the 71 kcal mol^{-1} suggested by Davis et al. through model clusters.[49] These authors, however, used calculations of triprotonated H_3PM_{12} clusters to determine a reliable proton affinity difference between the bridging oxygens in PMo_{12} and PW_{12} of 9 kcal mol^{-1}, a value that is similar to the ∼6 kcal mol^{-1} computed in the present work for the mixed tungstomolybdate cluster. When the proton attaches to a bridging oxygen, there is an additional stabilization via a hydrogen bond with the nearest bridging oxygen. In H−OMo_2, the H is bonded to OMo_2 with a bond length of 0.99 Å and the distance to OW_2 is 2.03 Å. The conformation with the H oriented away from the molecular framework is notably higher in energy, more than 10 kcal mol^{-1}. This additional stabilization is similar in H−OMo_2 and H−OW_2 and, therefore, does not modify their relative stability, but it is an important factor in the difference of affinity between a proton residing on a terminal and in a bridging oxygen.

Solvent Effects. In the discussions above, we have implicitly assumed that the anions were in the gas phase with neither

(47) Kempf, J. Y.; Rohmer, M.-M.; Poblet, J.-M.; Bo, C.; Bénard, M. *J. Am. Chem. Soc.* **1992**, *114*, 1136.
(48) Okuhara, T.; Mizuno, N.; Misono, M. *Adv. Catal.* **1996**, *41*, 113.
(49) Bardin, B. B.; Bordawekar, S. V.; Neurock, M.; Davis, R. J. *J. Phys. Chem. B* **1998**, *102*, 10817−10825.

Chart 1

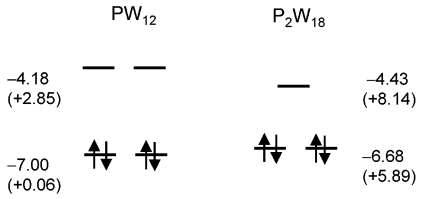

counterions nor solvent molecules. It is well known that highly charged title anions do not exist in the gas phase and that the external field generated by the counterions and the solvent is crucial to stabilize the POMs. In solution, many of the properties of the POMs depend on the concentration, the ionic strength, the pH of the solution, and so forth. At present, it is still not possible to take all these factors into account in a quantum chemistry study. However, a first-order approximation for dilute solutions is to model the solvent effect by a polarizable continuum.[30] Let us take, for example, the Keggin anion $[PW_{12}O_{40}]^{3-}$. In the gas phase, the molecular orbitals are very high in energy because of the large negative charge of the anion. In general, POMs may be viewed as a neutral cage encapsulating an anion in its interior;[1,8] this is the so-called clathrate model that allows $[PW_{12}O_{40}]^{3-}$ and $[P_2W_{18}O_{62}]^{6-}$ to be reformulated as $[PO_4]^{3-}@W_{12}O_{36}$ and $[PO_4]_2^{6-}@W_{18}O_{54}$, respectively. The unoccupied metallic band of the *neutral* $W_{12}O_{36}$ and $W_{18}O_{54}$ cages appears very low in energy. The LUMO lies near −6.5 eV in both frameworks. The encapsulation of the phosphate anions in the interior of the neutral cages shifts all the molecular orbitals of the POM toward higher energies. Hence, the absolute energies of the frontier orbitals in the 1:12 tungstate are +0.06 eV and +2.85 eV, respectively. If $W_{12}O_{36}$ encapsulates a silicate, with a charge of −4, the shift is even more considerable but the H−L gap is still independent of the total charge of the encapsulated anion. We kept in mind that POMs are *easily reducible* chemical species and, therefore, the energy of the lowest unoccupied orbitals must be low enough to accept the incoming electron. The crystal field in the solid state[50] and the solvent molecules in dilute solutions stabilize the anion, placing the molecular orbitals at the appropriate level. Chart 1 gives the energy of some frontier orbitals for several clusters in water solution and gas phase (in parentheses). There is a considerable decrease in MO energies after the solvation and the magnitude of this decrease parallels the charge of the anion. In Chart 1, the lowest metallic orbitals and particularly the LUMO appear at quite negative energies (about −4 eV). This is a *necessary* condition for an easy reduction.

It is well known that although P_2W_{18} has a larger charge it is more oxidant than PW_{12}. In the gas phase, the process

$$[PW_{12}\ 1e]^{4-} + [P_2W_{18}]^{6-} \rightarrow [PW_{12}]^{3-} + [P_2W_{18}\ 1e]^{7-}$$

is highly endothermic ($\Delta E = +5.07$ eV) because, in absolute value, the LUMO in the W−D anion has much greater energy. Consequently, in the absence of external fields, the extra electron simply prefers to go to the least charged Keggin anion. Otherwise, in solution, the frontier orbitals have similar energies (Chart 1) and the process becomes slightly exothermic ($\Delta E = -0.11$ eV). We checked whether the inner reduction properties

(50) Maestre, J. M.; Sarasa, J. P.; Bo, C.; Poblet, J.-M. *Inorg. Chem.* **1998**, *37*, 3071.

Chart 2

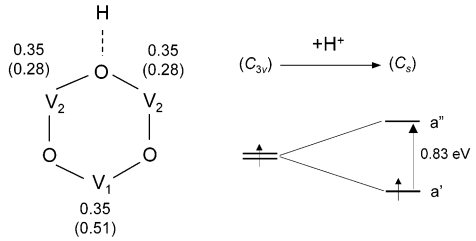

of W−D anions are affected by the solvent. The difference in the stability of a P_2W_{18}1e reduced at a polar site and a P_2W_{18}-1e reduced at an equatorial site is not altered by the presence of the solvent. We also did not observe any difference in the relative stability of the reduced anions of the mixed cluster $P_2W_{15}V_3$. These results are consistent with the almost isotropic field generated by the continuum model that modifies the absolute MO energies but does not change their relative values. Therefore, in the absence of short intermolecular contacts, the *study of isolated anions* is enough to understand many redox properties of POMs. Often, the properties of a POM may simply be described by the electronic properties of the corresponding neutral cage; for example, the difference in the reduction energy between the polar and equatorial sites in the neutral cage $W_{18}O_{54}$ was computed to be 0.71 eV, a value that is very similar to the energy difference computed for the complete cluster $[PO_4]_2^{6-}@W_{18}O_{54}$, 0.84 eV.

Finally, we shall briefly discuss the effect of protonation on the redox properties of a POM. In particular, we reanalyzed the reduction of the tungstovanadate SiW_9V_3 after protonation of one of the bridging OV_2 oxygens. In the unprotonated species, the reduction involves the addition of one electron to a degenerate orbital delocalized over the three vanadium centers. Because of the C_{3v} molecular symmetry, the three vanadiums are equivalent and so the metallic electron is equally shared with a spin population of 0.35 e per vanadium. The protonated form retains only one symmetry plane, and so the doubly degenerate LUMO in the unprotonated form splits into two orbitals of symmetry a′ and a″. Orbital a′ is 0.83 eV lower in energy than a″ and has a larger participation of the V_2 d-orbitals (Chart 2). As a result, the reduction yields an asymmetric distribution of the spin density between the three vanadiums, 0.28 e (V_2) and 0.51 e (V_1). In summary, the protonation process changes the chemical nature of the V-substituted part of the molecule, making the vanadium atoms different from one other.

Conclusions and Summary

DFT calculations were carried out on a series of mixed Keggin and Wells−Dawson (W−D) anions so that their redox and basicity properties could be analyzed. The unoccupied metallic orbitals of POMs without paramagnetic ions, in general, and these anions, in particular, are well separated in energy from the band of occupied oxo orbitals. Two factors govern the redox properties of a POM: the energy and composition of the lowest unoccupied orbitals, formally symmetry-adapted d_{xy}-type orbitals developed on the addenda atoms, and the total charge of the anion. In an α-XM_{12} anion, all metals are equivalent, and so they all have the same probability of trapping the additional electron when the cluster is reduced. When the ion W^{6+} in the 1:12 tungstate is substituted by a more electronegative Mo^{6+} ion, the energy of the LUMO decreases and the cluster is more

easily reduced, the additional electron going to a Mo orbital. The same phenomenon takes place when a V^{5+} replaces a W^{6+}: the extra electron goes to the vanadium center. Mixed tungstoniobates behave differently since niobium orbitals are inserted into the tungsten band and the reduction of SiW_9Nb_3, for example, yields the *blue* species SiW_9Nb_3 1e and not the cluster $SiW_9Nb^V2Nb^{IV}$.

W−D P_2M_{18} structures formally consist of two PM_9 halves linked by almost linear M−O−M bonds (∼162°). In the most compact Keggin anion, all M−O−M angles range between 125 and 150°. This structural difference determines the electronic and redox properties of the W−D anions. The LUMO in P_2W_{18} is an orbital that is formally delocalized over the belt addenda atoms. Consequently, the reduction preferentially occurs in the belt sites. The alternative reduction on the cap sites requires 0.84 eV more. For the analogous 2:18 molybdate, the reduction is shifted to lower potentials and the difference in the reduction energy between the polar and equatorial sites is somewhat lower, 0.69 eV. When three V's replace the three polar W's in one-half of the P_2W_{18} anion, two factors strongly compete to capture the additional electron in the reduced species: the *most favorable equatorial position* and the *higher electron affinity* of ion V^{5+}. In $P_2W_{15}V_3$, the chemical factor is the dominant one and the reduction occurs in the vanadium center located at the cap site. If molybdenums occupy the cap sites, the competition between those two factors is heavier.

The bridging oxygens are the most basic sites in single-addenda and mixed Keggin anions. The calculations carried out on protonated forms of the mixed clusters SiW_9V_3 and SiW_9Mo_3 suggest the following basicity scale for the various terminal and bridging oxygen types: OV_2 > OMo_2 > OW_2 > OV > OW > OMo. The difference in the proton affinity between the terminal and bridging oxygens ranges between 6 and 32 kcal mol^{-1}.

Many POMs can be considered as supramolecular species since the host cage and the encapsulated guest are clearly identifiable.[51] Lindqvist, Keggin, and W−D structures have also been formulated as clathrate structures[8] like $O^{2-}@[M_6O_{18}]^{(m-2)-}$, $[XO_4]_2{}^{n-}@[M_{12}O_{36}]^{(m-n)-}$, and $[XO_4]_2{}^{n-}@[M_{18}O_{54}]^{(m-2n)-}$ but the POM cage encapsulates an anion that is perfectly inserted into the octahedral environment of metal atoms and their consideration as encapsulation compounds is, therefore, more arbitrary. However, this description enabled the thermodynamics of the α and β isomers of the Keggin anions to be rationalized.[19] The clathrate model also helps to describe the various factors that govern the redox properties of a POM. For example, the unoccupied metallic band of the neutral cage $[W_{12}O_{36}]$ appears very low in energy (about −6.5 eV) and this is a *necessary* condition for a molecule to be easily reducible. When the POM cage encapsulates an anion in its interior, all the MOs of the POM are strongly shifted toward higher energies and this shift increases with the charge of the anion. The external field—generated by the counterions and solvent molecules in solution and solid state—restores the metallic band of the POM to the appropriate level and allows the POM to be reduced easily. Despite this intrinsic complexity, the simple analysis of the neutral cage often enables the properties of a polyoxoanion to be rationalized. Hence, for instance, the energy difference in reduction between the polar and equatorial sites in a W−D anion in solution is reproduced from the $[M_{18}O_{54}]$ cage in the gas phase. For anions with different total charges to be effectively compared, however, external fields must be included in the calculations. Using a continuum model for the solvent, we compared the oxidizing power of $[PW_{12}O_{40}]^{3-}$ and $[P_2W_{18}O_{62}]^{6-}$. The incorporation of the solvent in the calculations by means of a *continuum* model represents a first step in the analysis of the stabilizing effects produced by the external field on the anion. Studies are underway to include the water molecules explicitly in the calculations by means of molecular dynamics in combination with the DFT methodology. We hope that in the near future the better knowledge of the role that the solvent molecules and the counterions play in the polyoxometalate chemistry will allow computing absolute redox potentials as well as absolute protonation energies.

Acknowledgment. All the calculations have been carried out on workstations purchased with funds provided by the DGICYT of the Government of Spain and by the CIRIT of Generalitat of Catalunya (Grants n° PB98-0916-C02-02 and SGR01-0315). We thank Y. Jean and L. Nadjo for sharing the information of their unpublished work. We also thank the referees for their comments and suggestions.

Supporting Information Available: The computed *xyz* coordinates for several structures. This material is available free of charge via the Internet at http://pubs.acs.org.

JA020407Z

(51) Müller, A. *Nature* **1991**, *352*, 115. Müller, A.; Peters, F.; Pope, M. T.; Gatteschi, D. *Chem. Rev.* **1998**, *98*, 239.